Overview of the RFX-mod Fusion Science Activity

M. Zuin[1], S. Dal Bello[1], L. Marrelli[1], M.E. Puiatti[1], P. Agostinetti[1], M. Agostini[1], V. Antoni[1], F. Auriemma[1], M. Barbisan[1], T. Barbui[1], M. Baruzzo[1], F. Belli[2], P. Bettini[1], M. Bigi[1], R. Bilel[1], M. Boldrin[1], T. Bolzonella[1], D. Bonfiglio[1], M. Brombin[1], A. Buffa[1], C. Bustreo[1], A. Canton[1], S. Cappello[1], L. Carraro[1], R. Cavazzana[1], D. Cester[3], L. Chacon[4], G. Chitarin[1], W.A. Cooper[6], L. Cordaro[1], M. Dalla Palma[1], S. Deambrosis[7], R. Delogu[1], A. De Lorenzi[1], G. De Masi[1], J.Q. Dong[8], D.F. Escande[9], A. Fassina[1], F. Felici[29], A. Ferro[1], C. Finotti[1], P. Franz[1], L. Frassinetti[10], E. Gaio[1], F. Ghezzi[11], L. Giudicotti[1], F. Gnesotto[1], M. Gobbin[1], W.A. Gonzalez[1], L. Grando[1], S.C. Guo[1], J.D. Hanson[12], S.P. Hirshman[4], P. Innocente[1], J.L. Jackson[13], S. Kiyama[14], M. Komm[15], O. Kudlacek[1], L. Laguardia[11], C. Li[26], B. Liu[1], S.F. Liu[16], Y.Q. Liu[17], D. López- Bruna[27], R. Lorenzini[1], T.C. Luce[13], A. Luchetta[1], A. Maistrello[1], G. Manduchi[1], D.K. Mansfield[18], G. Marchiori[1], N. Marconato[1], D. Marcuzzi[1], P. Martin[1], E. Martines[1], S. Martini[1], G. Mazzitelli[2], O. McCormack[1], E. Miorin[5], B. Momo[1], M. Moresco[1], Y. Narushima[28], M. Okabayashi[18], R. Paccagnella[1], N. Patel[1], M. Pavei[1], S. Peruzzo[1], N. Pilan[1], L. Pigatto[1], R. Piovan[1], P. Piovesan[1], C. Piron[1], L. Piron[1], I. Predebon[1], G. Pucella[2], C. Rea[1], M. Recchia[1], A. Rizzolo[1], G. Rostagni[1], C Ruset[19], L. Sajò-Bohus[20], H. Sakakita[14], R. Sanchez[4,21], J.S. Sarff[5], F. Sattin[1], P. Scarin[1], O. Schmitz[22], W. Schneider[25], M. Siragusa[1], P. Sonato[1], E. Spada[1], S. Spagnolo[1], M. Spolaore[1], D.A. Spong[4], G. Spizzo[1], L. Stevanato[3], Y. Suzuki[28], C. Taliercio[1], D. Terranova[1], O. Tudisco[2], G. Urso[23], M. Valente[1], M. Valisa[1], M. Vallar[1], M. Veranda[1], N. Vianello[1], F. Villone[24], P. Vincenzi[1], N. Visonà[1], R.B. White[18], P. Xanthopoulos[25], X.Y. Xu[1], V. Yanovskiy[1], A. Zamengo[1], P. Zanca[1], B. Zaniol[1], L. Zanotto[1], Y. Zhang[1] and E. Zilli[1]

[1] Consorzio RFX, Corso Stati Uniti 4, 35137 Padova, Italy
[2] Centro Ricerche Energia ENEA Frascati, Frascati, Italy
[3] Dipartimento di Fisica e Astronomia, Università degli Studi di Padova, Padova, Italy
[4] ORNL Fusion Energy Division, Oak Ridge, TN, USA
[5] Department of Physics, University of Wisconsin, Madison, WI, USA
[6] EPFL, Centre de Recherches en Physique des Plasmas, Lausanne, Switzerland
[7] CNR-IENI, Corso Stati Uniti 4, 35127 Padova, Italy
[8] Institute for Fusion Theory and Simulation, Zhejiang University, Hangzhou, Southwestern Institute of Physics, Chengdu, People's Republic of China
[9] Aix-Marseille Universitè, CNRS, PIIM, UMR 7345, Marseille, France
[10] Royal Institute of Technology KTH, SE-10044 Stockholm, Sweden
[11] CNR-IFP, Via R. Cozzi 53 20125 Milan, Italy
[12] Physics Department, Auburn University, Auburn, AL, USA
[13] General Atomics, PO Box 85608, San Diego, CA 92186-5608, USA
[14] Plasma Frontier Group, Energy Technology Research Institute, National Institute of Advanced Industrial Science and Technology (AIST), Tsukuba, Ibaraki 305-8568, Japan
[15] Institute of Plasma Physics, Czech Academy of Sciences, Prague, Czech Republic
[16] Department of Physics, Nankai University, Tianjin 300071, People's Republic of China
[17] CCFE Fusion Association, Culham Science Centre OX14, Abingdon, Oxfordshire, UK
[18] Princeton Plasma Physics Laboratory, Princeton, NJ, USA
[19] National Institute for Laser, Plasma and Radiation Physics, Association Euratom-MEdC, Bucharest, Romania
[20] Universidad Simon Bolivar, Nuclear Physics Laboratory, Caracas, Venezuela
[21] Universidad Carlos III de Madrid, Madrid, Spain
[22] Department of Engineering Physics, University of Wisconsin-Madison, Madison, WI, USA
[23] CNR, Istituto Per le Applicazioni del Calcolo 'M. Picone', Roma, Italy
[24] Consorzio CREATE, DAEIMI, Università di Cassino, Cassino, Italy
[25] Max-Planck-Institut fur Plasmaphysik, Teilinstitut Greifswald, 17491 Greifswald, Germany
[26] University of Science and Technology of China, Hefei, Anhui, People's Republic of China

[27] Laboratorio Nacional de Fusiòn, CIEMAT, Avenida Complutense 22, 28040 Madrid, Spain
[28] National Institute for Fusion Science, 322-6 Oroshi-cho, Toki 509-5292, Japan
[29] Department of Mechanical Engineering, Control Systems Technology Group, Eindhoven University of Technology, PO Box 513, 5600 MB Eindhoven, The Netherlands

Mail to: matteo.zuin@igi.cnr.it

Abstract. This paper reports the main recent results of the RFX-mod fusion science activity. The RFX-mod device is characterized by a unique flexibility in terms of accessible magnetic configurations. Axisymmetric and helically shaped Reversed-field pinch equilibria have been studied, along with tokamak plasmas in a wide range of q(a) regimes (spanning from 4 down to 1.2 values). The full range of magnetic configurations in between the two, the so-called ultra low-q ones, has been explored, with the aim of studying specific physical issues common to all equilibria, such as, for example, the density limit phenomenon. The powerful RFX-mod feedback control system has been exploited for MHD control, which allowed to extend the range of experimental parameters, as well as to induce specific magnetic perturbations for the study of 3D effects. In particular, transport, edge and isotope effect in 3D equilibria have been investigated, along with runaway mitigations through induced magnetic perturbations. The first transitions to an improved confinement scenario in circular and D-shaped tokamak plasmas have been obtained thanks to an active modification of the edge electric field through a polarized electrode. The experiments are supported by intense modelling with 3D MHD, gyrokinetic, guiding center and transport codes. Proposed modifications to the RFX-mod device, which will enable further contributions to the solution of key issues in the roadmap to ITER and DEMO, are also briefly presented.

1. Introduction

The RFX-mod device (2m and 0.46m major and minor radii, respectively), thanks to its flexibility and unique control capability due to the advanced MHD-control feedback system, made of 192 independently driven active coil, is operated to investigate a wide range of experimental conditions [1].
Reversed-Field Pinch (RFP), tokamak and the full range of magnetic configurations in between the two, the so-called ultra-low q (Ulq) ones, are produced to investigate common physics topics and highlight both similarities and peculiarities. The RFX-mod scientific program provides a complementary contribution to tokamak and stellarator physics on fundamental aspects, including 3D effects, transport barriers and MHD control. The experiments are inspired and complemented by an intense theoretical and modelling activity, in particular to understand the effects of a helical boundary.

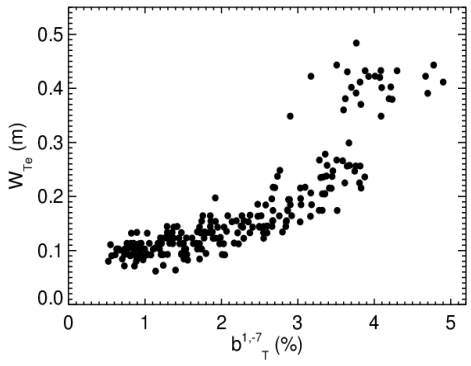

Fig.1: ITB width W_{Te} vs the normalized amplitude of the dominant helical perturbation, $b^{1,-7}$.

The RFP is characterized by comparable toroidal and poloidal fields (q(r) < 1) and by the edge toroidal field reversal (q(a) < 0), so that, unlike configurations with large toroidal field, the magnetic field strength in the RFP is minimum at the magnets.
The other operating RFP experiments are MST in the USA, Extrap-T2R in Sweden, RELAX in Japan and the newly built KTX in PRC.
As a RFP, RFX-mod is devoted to an experimental and modelling effort to deepen the understanding of the confinement properties at high current (up to 2MA).
High current regimes in RFX-mod have indeed been proved to be dominated by a self-organization process due to the action of one toroidal mode in the tearing spectrum, which breaks axisymmetry and induces the formation of a helical structure in the plasma core. The spontaneous tendency of RFP plasmas towards the so-called quasi-single helicity (QSH) state has been observed in other RFP devices. In MST [2], as in RFX-mod, such condition is more frequent in discharges with a RFP equilibrium

characterized by a toroidal magnetic field at the edge very close to zero (shallow reversal) and at high Lundquist numbers, while in the low-aspect-ratio RELAX device QSH states have been observed also in deeply reversed discharges [3].

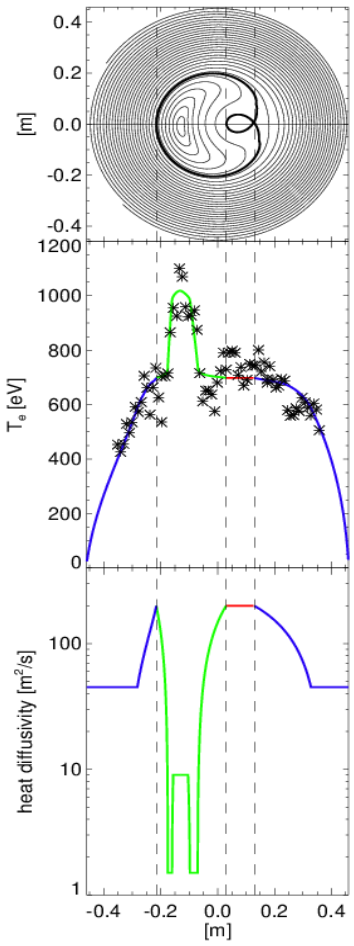

Fig. 2: From the top: Flux surface reconstruction for a DAx plasma; electron temperature profile (dots refer to experimental values, the solid line to the reconstructed T_e profile); heat diffusivity profile computed by MAxS. Different colors refer to the various domains considered in the analysis.

The studies on the formation and the effects of the electron transport barriers developing in the single helical axis (SHAx) states have been extended in RFX-mod, evaluating the confinement and transport properties, the edge response, and the isotope effects in 3D equilibria conditions.

The role of a helical boundary in the formation of 3D core equilibria in toroidal plasmas has been analyzed, focusing in particular on its impact on the current density profile through dynamo mechanisms. The results of experiments in RFX-mod have been compared with those recently performed in tokamak plasmas in hybrid regime and with the predictions of dedicated modelling with visco-resistive linear and nonlinear 3D MHD codes. Moreover, following the results from such MHD models, experiments have been performed in helical regimes stimulated by non-resonant magnetic perturbations.

The experiments performed in RFP, tokamak and Ulq forced the development of analysis activities aimed at deepening the comprehension of the density limit phenomenon in all configurations.

In the last experimental campaign, the first H-modes in shaped and circular tokamak plasmas have been obtained thanks to an inserted edge polarized electrode. The formation of an edge pedestal has been characterized by insertable probes.

Based on the achievements of the last years and in order to extend the explored parameter range and the capability to contribute to the general advancement in fusion science some upgrades are planned, whose technical design is presently in the final phase and which will be also briefly presented.

2. 3D effects in RFP and tokamak plasmas

2.1. Internal transport barriers and helical state formation

In the RFP the resonant tearing modes sustaining the configuration cause field line reconnection and make the magnetic field stochastic. However, when a single resonant mode, with m = 1 and n = −7 in RFX-mod (hereafter, couples of m>0 and n<0 indicate modes resonant inside the reversal surface in RFP plasmas) dominates the spectrum of the secondary instabilities, the separatrix of the island associated to this mode is expelled, and the island O-point becomes the new single helical axis of the plasma (SHAx state).

In this condition, the effect of field stochasticity and the associated anomalous transport are mitigated [4,5]. In RFX-mod, SHAx plasmas feature steep electron temperature gradients, interpreted as internal transport barriers (ITBs). Such ITBs enclose helical thermal structures, which are not penetrated by (heavy and light) impurities as the result of strong outward impurity convection. The experimental evidence of impurity outward convection in RFX-mod found in the past in Ni LBO and Ne gas puffing experiments [6] has been confirmed by C and Li solid pellets experiments [7], by recent Ne doped D_2 cryogenic pellet injection and also by W LBO injections. Similar diffusion coefficient and outward convection resulted from the impurity transport analysis of all the considered impurity species, without strong dependence on mass/charge. Instead, a strong convection has not been found for the main gas [8] and a favorable situation with peaked or flat density profiles and hollow impurity profiles is produced.

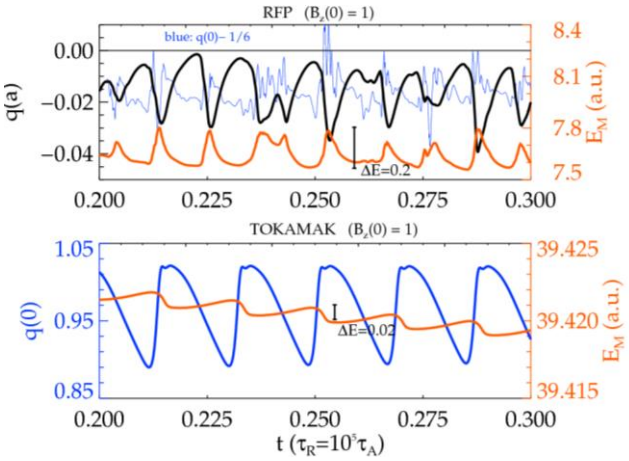

Fig. 3: Top: Edge safety factor and magnetic energy time behaviour from 3D nonlinear MHD modeling for the RFP case. Bottom: Core safety factor and magnetic energy time trace for the tokamak case.

In RFX-mod, the width of thermal structures enclosed by ITB, W_{Te}, features an increasing trend with the dominant mode amplitude, as shown in Fig. 1. Such a trend is continuous and smooth even at the inverse saddle-node bifurcation, when the plasma enters the SHAx state. It has been recently shown that a key role on the barrier radial extension is played by the level of the increased stabilization of secondary modes occurring as the dominant one increases [9,10]. It is worth to note that this result provides positive expectations for future RFP plasmas with enhanced heating since secondary modes have been shown to be stabilized by increasing the Lundquist number, as confirmed by theoretical predictions [10,11].

The understanding of the confining properties of the RFP configuration in the presence of one or several islands embedded in the main plasma, each with its own magnetic axis, requires to quantify to which extent the island modifies transport, i.e. the estimation of the energy and particle transport coefficients also inside and around the island.

A fast and usual way to calculate the effective transport coefficients is based on well-developed 1.5D transport codes (e.g. ASTRA, CRONOS, JETTO and others). However, such codes are applicable only for closed flux surfaces nested around a single axis and their application to situations where the magnetic resonances develop into islands is prevented. Recently, a multiple axis solver (MAxS) able to treat plasmas with islands in 1.5 dimensions has been developed, based on a Multiple Domain Scheme (MDS) [12,13]. The MAxS code has been successfully used to interpret RFP plasmas in both double axis (DAx , configuration where the island separatrix has not been expelled) and SHAx states in RFX-mod. In Fig. 2, an example is given of the results

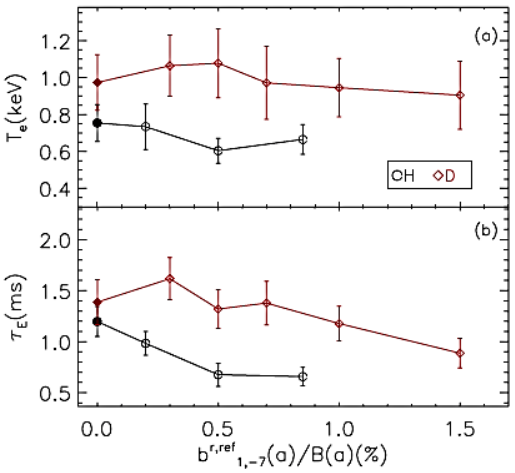

Fig. 4: (a) Average core T_e versus the normalized $b_{1,-7}$ amplitude in hydrogen (black) and deuterium (red) plasmas. (b) Average energy confinement time τ_E.

for the heat diffusivity profile obtained for a DAx case. The code has been also applied to model transport properties of the Large Helical Device (LHD) and TJ-II Heliac plasmas [12].
3D nonlinear magnetofluid modelling by SpeCyl and PIXIE3D codes [17] highlights a series of parallelisms between the RFP and the tokamak configurations, as far as the dynamical evolution of helical states is studied. The first is given by the oscillatory behavior of the magnetic field, usually associated to the growth of plasma instabilities typically ending in a reconnection event where magnetic energy is converted into kinetic one, as recently experimentally observed [14] and shown in Fig. 3: what changes is only the shape and amplitude of the kink modes involved in the process. In Fig. 3, it can be noted that the release of magnetic energy in the RFP relaxation is up to two orders of magnitude larger than in the tokamak, when considering configurations with the same core value of Bz. The corresponding oscillations in the core and edge q values are shown in the same figure.

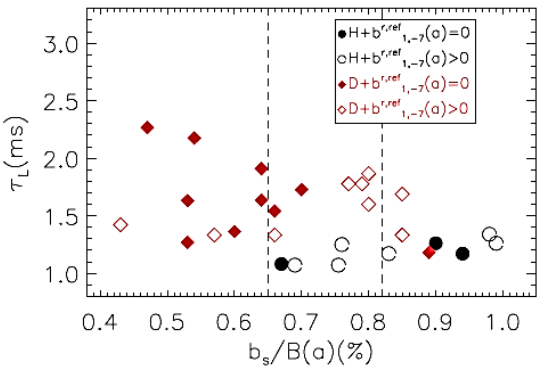

Fig. 5: Helical loss time versus secondary modes amplitude for standard (full symbols) and induced (empty symbols) helical deuterium (red diamonds)/ hydrogen (black circles) discharges.

Note that in the RFP case the resonance of the mode 1/-6 (non-resonant on average) is quasi-periodically touched in the dynamical evolution. Simulations show that mitigation of sawtoothing activity can be observed at higher dissipation (resistive or viscous [15]) and when imposing a small edge helical modulations of the magnetic boundary, called magnetic perturbations (MPs) [16]. MPs provide sawtoothing mitigation by conveying the system to steady nonlinear saturation of the kink modes: the RFP becomes a global quasi-helical configuration while the tokamak is characterized by the presence of a stationary helical state in the core (snake-like) [17,18]. 3D modelling also predicts that the helical core distortion can redistribute the central current, thus modifying the q-profile, through a dynamo mechanism, which has important impact on MHD stability and confinement properties.

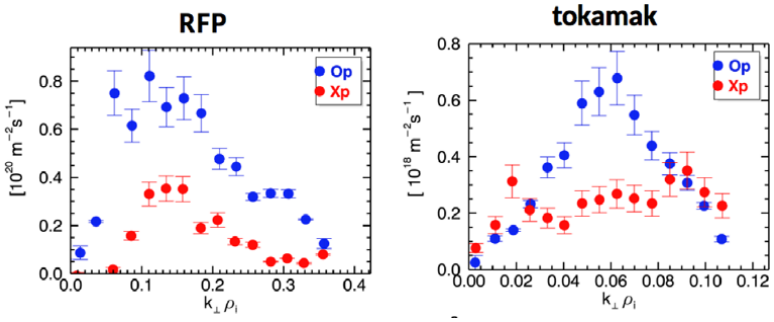

Fig. 6: k-resolved particle flux for RFP and tokamak plasmas. Blue and red dots refer to data on the O- and X-point respectively.

In the RFP, in SHAx states, plasma rotation assumes a helical pattern, which, associated to the internal 3D field, produces an effective negative dynamo loop voltage. MHD modelling reveals that the helical displacement causes a modulation of the parallel current along each flux tube, associated to an electrostatic potential, giving rise to the observed dynamo flow [19]. This observation remains valid when studying helical states in tokamaks, in particular when the deformation produced by the 2/1 tearing mode and the internal 1/1 mode is considered. Experiments performed in RFX-mod tokamak plasmas confirmed the predictions [20]. These results have been proved to be relevant also for high-β DIII-D plasmas when a helical core forms induced by an external n=1 MP and can explain the observed central current redistribution [21]

2.2. Isotope effect on 3D plasmas

Experiments have been performed to investigate the role of the ion mass M_i on plasma dynamics in the RFP. Interestingly, the existing main magnetic configurations are characterized by largely different responses to the change of the working gas. While no clear isotope effect has been documented in non axi-symmetric devices like stellarators [22], in tokamaks a positive isotope effect is experimentally observed in terms of confinement properties with increasing ion mass. The reduction of anomalous transport in the tokamak has been to our knowledge only qualitatively well reproduced in numerical modelling of collisional drift waves [23] and dissipative trapped electron modes induced turbulence [24], also considering the effect of non-adiabatic electron response, electron–ion collisions and impurities [25].

The RFP, indeed, allows the exploration of a space of plasma parameters complementary to those of tokamaks and stellarators and gives a unique possibility to gain more insight into the isotope effect physics, by comparing axisymmetric and helical equilibria.

In the RFP, the isotope effect has been evidenced in a variety of aspects. A positive dependence approximately as the square root of the ion mass is found for the non-collisional ion heating during magnetic reconnection processes in MST [26], strongly involving also impurities [27] and associated to the generation of non-maxwellian ion tails [28]. The ion mass is also found to influence the penetration of neutrals in the core, which is smaller in deuterium plasmas than in hydrogen plasmas [29], as well as to determine the rotation velocity and braking curves of tearing modes [30].

In RFX-mod a clear isotope effect is observed on the magnetohydrodynamic properties of RFP plasmas by comparing hydrogen and deuterium discharges. Increasing Mi brings about a stabilizing effect on tearing modes, producing longer SHAx states, more monochromatic and more resilient to weak sawtoothing. The measured electron temperature is higher in deuterium than in hydrogen in a significant fraction of the plasma volume (r/a<0.9) and the energy confinement time scales $\sim Mi^{0.3}$. The particle influx is significantly reduced and the particle confinement time shows a scaling $\sim Mi^{0.45}$. Such effect on confinement has been mainly associated to the mitigation of transport at the edge, internally to the scrape-off layer where long range correlations have been detected [31].

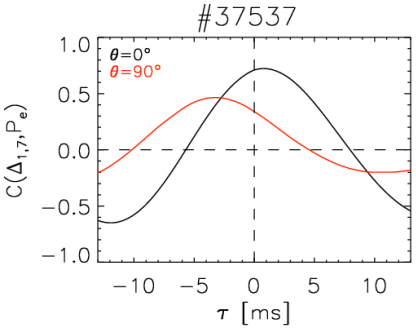

Fig. 7: Cross-correlation between electron pressure and local m=1 magnetic shift at two poloidal angles in the RFP. A different phase relation between the two indicates a not pure m=1 pressure perturbation.

3D magnetic fields have been applied both in H and D [32]. Only a slight effect of such perturbations has been observed on the confinement properties, as shown in Fig. 4, where the core electron temperature T_e and the estimated energy confinement time τ_E are shown as a function of the normalized amplitude of the applied 3D field for the two isotopes. Such behaviour has been numerically investigated by the Hamiltonian guiding center code ORBIT, with attention to the magnetic topology in plasmas with and without the application of 3D fields on deuterium and hydrogen test ion transport. In agreement with experimental estimates, numerical studies show that particle transport is reduced in deuterium plasmas but not significantly affected by the application of helical boundary conditions. This result is summarized in Fig. 5, where the estimated helical loss times are reported as a function of the normalized amplitude of the secondary modes, $b_s/B(a)$.

2.3. 3D properties of edge plasma

The interaction between a 3D magnetic field and the kinetic properties of the plasma edge is a topic of growing interest in the fusion community. The presence of magnetic islands close to the edge and the application of magnetic perturbations strongly modify the edge region of fusion experiments, impacting on the overall performance of the discharges. In particular, MPs in tokamaks and stellarators are used to control the plasma wall-interaction, to reduce the power fluxes to the divertor plates, to mitigate or suppress ELMs, and for runaway electron control. However, the action of MPs on the edge plasma is far from being well understood, so that detailed studies have been recently performed aimed at the characterization of the kinetic response of the edge plasma to a 3D magnetic field with different helicity in the RFX-mod experiment, operated both in RFP and tokamak configurations to study plasmas in different configurations in the same device with the same diagnostics [33,34,35]. In the presence of rotating magnetic perturbations the measured time evolution of plasma parameters indicates that the profiles of electrostatic particle and energy flux mainly follow the symmetry of the dominant imposed perturbation. The electrostatic turbulence induced flux is modulated by the underlying topology, with an enhancement close to the O-point and a reduction at the X-point of the (spontaneous or induced) magnetic island.

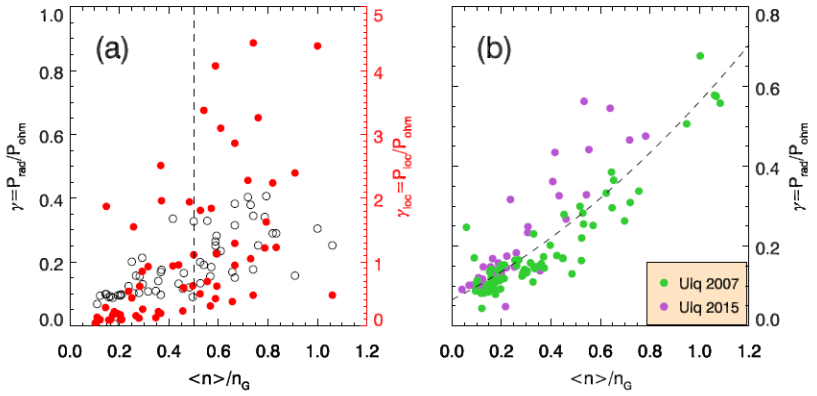

Fig. 8: P_{rad}/P_{Ohm} ratio as a function of normalized density: a) RFP case, b) Ulq plasmas. In a) black points refer to global values, red ones to values from a local balance along the toroidal angle.

It is important to underline that this major result has been found to be independent of the adopted magnetic configuration: the modulation of flux profiles manifests itself with an increase around the O-point of the outermost resonating island and a reduction in the X-point region due to the fluctuation level and not to the relative phase between electron density and electric field fluctuations.

In terms of transport relevant k, an analysis of the spectra of the fluxes reveals that the transport contribution is due to fluctuations propagating in the electron diamagnetic drift direction peaked at $k_{perp}\rho_i \sim 0.1$ in the RFP case (at a plasma current, I_p, around 400kA) and at $k_{perp}\rho_i \sim 0.06$ in the tokamak case (with I_p<150kA), as is shown in Fig. 6, where the k-resolved spectra of the electrostatic particle flux is shown for both magnetic configurations.

Moreover, for different MPs in both RFP and tokamak equilibria, the behaviour of the edge plasma profiles has been characterized, studying the detailed behaviour of edge floating potential V_f along the poloidal angle with the internal array of electrostatic sensors (ISIS). In the RFP the electron pressure P_e has been also measured along the poloidal direction with the Thermal Helium Beam (THB). The refined analysis has highlighted that the edge properties are actually modulated by a richer spectrum, where additional harmonics on top of the dominant one must be taken into account for both RFP and tokamak equilibria. Especially along the poloidal angle, in the RFP the edge plasma has not a pure m=1 structure, since its modulation is due to the mutual interaction of the m=1 and m=0 modes.

An analysis of the connection length, L_{cw}, to the wall has shown that also this quantity does not exhibit a pure m=1 behaviour. The non-genuine m=1 structure of the connection length gives a strong hint that L_{cw} controls the structure of the floating potential and of the edge

electron pressure, which do not follow perfectly the m=1 island rotation [33]. This is visible in Fig. 7, where the correlation between P_e and the local magnetic shift is found to be a function of the poloidal angle. This result should be a caveat for MP application in tokamaks, because it shows that toroidal and poloidal sidebands can have a sizable effect on the kinetic response of the edge plasma.

2.4. Role of the magnetic topology on the density limit

It has been proved that the improved helical states in the RFP are observed at relatively low values of plasma density. A critical density value around $n/n_G = 0.35$ (with $n_G = I_p/\pi a^2$ the well-known empirical Greenwald density) is found to be an upper limit for the development of the helical states [36]. The reasons for this n/n_G limit are still under discussion. When the electron density further increases (above $n/n_G \sim 0.5$), the density profile becomes hollow and a MARFE-like radiative poloidal structure has been observed.

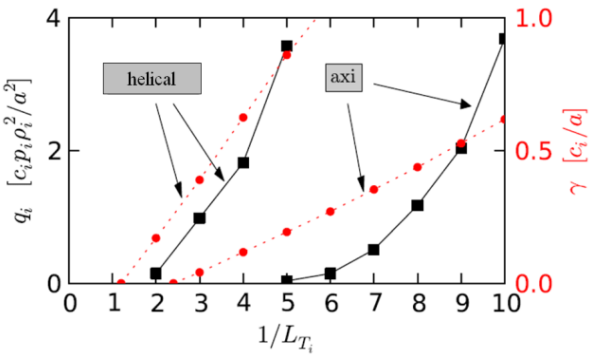

Fig. 9: Ion heat flux scaling as a function of the logarithmic ion temperature gradient ($1/L_{Ti}$), for the helical and the axisymmetric tubes. The linear growth rates (red) suggest the usual nonlinear shift, more pronounced in the axisymmetric case.

In [37] the results obtained in high density regimes in RFX-mod operated both as a tokamak and a RFP and in the FTU tokamak were compared. In FTU, the MARFE is an annulus of radiative-unstable plasma, which appears at $n0 > 0.4\ n_G$ [38] as a toroidal ring, poloidally localized. The threshold 0.4nG is consistent with the Lispschultz scaling of the MARFE critical density [39]. It was also shown that such toroidal MARFE is caused by a reduction of parallel electron conductivity, preventing energy redistribution along the flux surface, which induces the formation of local cold regions with strong line emission, on the high field side, where the core-originated heat flux is lower [40].

The scaling found in FTU is consistent with the nice, simple model proposed by Tokar [41] for the TEXTOR tokamak of this phenomenon, interpreted as a local imbalance between parallel heat diffusion and ionization/radial particle transport.

In RFX-mod RFP plasmas, radiation comes from He-like impurity lines (mainly O and C) excited by low temperatures in the formed edge poloidal annulus. No evidence of strong recombination has been deduced from the behaviour of the ratio of the H_γ / H_α lines along the toroidal angle [42].

The symmetry of the RFP MARFE is poloidal, which is easily explained, taking into account that the equilibrium field is poloidal in the RFP edge.

The MARFE in the RFP is toroidally localized and corresponds to a toroidal edge density accumulation strictly related to the magnetic topology, more specifically to the m=0 island chain resonant at the edge [37]. It has been proved, and successfully simulated via the guiding centre code ORBIT, that such density accumulation is due to an E×B convective cell arising as an ambipolar response of the plasma to the presence of the island fixed points.

To further test the essential role of the m=0 mode on the edge density limit occurrence, Ulq discharges have been produced and studied in high density conditions. Indeed, the Ulq equilibrium mainly differs from the RFP because of the absence of any m=0 resonance in the plasma. The results are shown in Fig. 8, where the measured P_{rad}/P_{Ohm} values are plotted as a function of the normalized electron density. In the RFP configuration, the localized MARFE is present well before the average density reaches the Greenwald value, $n=n_G$. In fact, when $n>0.5n_G$, the power radiated locally inside the MARFE greatly exceeds the local input power

(red dots in Fig.8(a)), even if globally $P_{rad}/P_{Ohm} < 0.5$ (open, black dots in Fig.8(a)). On the contrary, in Ulq discharges (see Fig.8(b)), the fraction of radiated power smoothly increases with n/n_G, with no localized radiative structure, being P_{rad}/P_{Ohm}~0.6 when n/n_G=1.0. Extrapolating the curve, one can obtain the theoretical balance $P_{rad}=P_{Ohm}$ for n/n_G~1.5, which is a value 3 times larger than the critical value for MARFE onset in the RFP.

2.5. 3D effects on microscale instabilities

The formation of ITB during SHAx states in the RFP stimulated the analysis of drift instabilities which could be destabilized by the existence of strong gradients at the plasma boundaries. Microtearing modes have been studied with gyrokinetic codes, also in low-collisionality regimes [43,44], and experimentally observed in RFX-mod [45].
It was also found that Trapped Electron Modes (TEM) may be driven unstable in RFP plasmas by density gradients much steeper than those required in tokamak plasmas, and which are found only at the very edge of profiles measured in the RFP plasmas in RFX-mod [46].

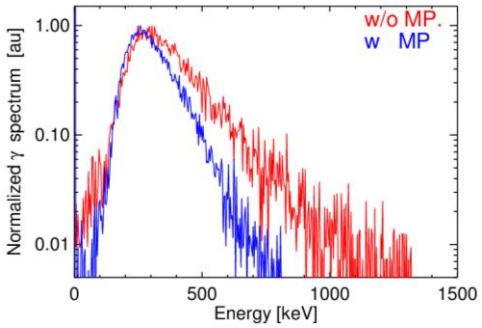

Fig. 10: Gamma ray spectra w/wo MP in RFX-mod tokamak plasmas.

In the past, the stability of the ion temperature gradient (ITG) mode was studied in the RFP with axisymmetric equilibrium models and the main conclusion from these geometrically simplified investigations was that the ITG stability threshold in the RFP was larger than in the tokamak, typically by a factor R/a (with R the major radius and a the minor radius of the torus). An explanation came from a detailed analysis of the parallel dynamics, showing a relevant Landau damping of the mode due to the short field connection length [47,48,49,50,51]. More recently, nonlinear simulations of ITG turbulence have been performed in order to revisit these findings. Turbulence induced by ITG has been investigated in the helical and axisymmetric plasma states of a RFP by means of gyrokinetic calculations with the massively-parallel Eulerian gyrokinetic code GENE [52], applied to the VMEC helical/axisymmetric RFP equilibria with the aid of the code GIST [53]. The two magnetic configurations have been systematically compared, both linearly and nonlinearly, in order to evaluate the impact of the geometry on the instability and its ensuing transport, as well as on the production of zonal flows. It has been demonstrated that, despite its enhanced confinement, the high-current helical state features a lower ITG stability threshold compared to the axisymmetric state. The results are summarized in Fig. 9, where the estimated linear ITG growth rate and the induced ion heat flux are plotted as a function of the ion temperature gradient at mid radius. While the linear growth rate (dotted lines) already suggests a sharp distinction between the two geometries, in a nonlinear environment their difference is even more pronounced (solid lines). ITG turbulence is thus expected to become an important contributor to the total heat transport in helical states with ITB.

2.6. Runaway mitigation through applied 3D magnetic perturbation

The possibility to de-confine runaway electrons, RE, and prevent their acceleration to high energies through the application of applied MP with different modal numbers and amplitude has been confirmed and further analyzed in dedicated experimental campaigns in RFX-mod operated as a tokamak. It has been proven that the application of proper MPs is indeed effective in preventing RE acceleration to very high energy, as shown in Fig. 10, where the normalized gamma ray spectra, measured by means of calibrated scintillators, exhibit a depression of the high energy component in the presence of MP. To interpret the RFX-mod

experimental results a relativistic version of the Hamiltonian guiding center code ORBIT has been developed [54]. The result of the analysis is summarized in Fig. 11, where the qualitative agreement is shown between the experimental data about the amplitude of the Hard X-ray signal and the normalized variation of RE energy $(\Delta E_k)_{norm}$ from the ORBIT simulation [54] when various MPs are applied. Such analysis recently suggested a successful experimental campaign on the ASDEX-U device, where a strong reduction of the post-disruption RE beam current has been obtained [55].

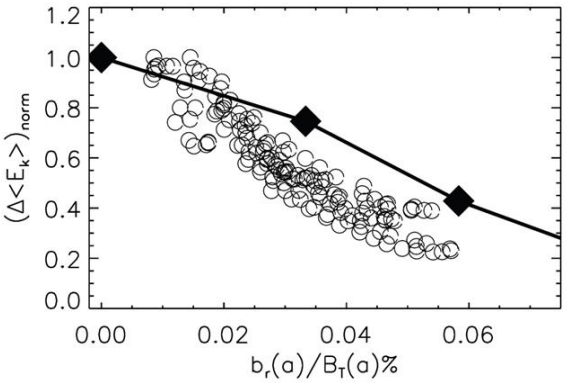

Fig. 11: The normalized variation of RE energy $(\Delta E_k)_{norm}$ from the ORBIT simulations (squares) compared with a subset of the data (circles) of the normalized Hard X-ray amplitude evaluated as a function of the normalized applied magnetic perturbation (from [54]).

3. Tearing mode dynamics studies

3.1. Locking-unlocking threshold of tearing mode with magnetic feedback in the RFP

Tearing modes, TM, in the RFP have the natural tendency to lock in phase together and to the wall [56]. Indeed, the image currents induced onto the wall develop a braking electromagnetic torque, which stops TM in the laboratory frame (wall-locking) as soon as their amplitude at the resonant surface exceeds a threshold (wall-locking threshold). When wall-locking occurs, the radial magnetic field penetrates the wall at a rate determined by the wall time-constant. Recent experiments in RFP plasmas demonstrated the possibility to recover the fast rotation branch of the tearing modes by lowering the plasma current under a certain threshold [56] (around 120 kA), corresponding to a low enough mode amplitude, and opened a new RFX-mod scenario characterized by the "natural" rotation of the dynamo modes. The experimental results, an example of which is given in Fig. 12, have been well reproduced by simulations performed with the validated MHD model RFXLocking code [56]. Such simulations demonstrate that the feedback action impeding the radial field penetration into the passive structure allows the recovery of the fast rotation with no hysteresis when reducing mode amplitude. This evidence changes the standard paradigm valid in the absence of feedback, which considers the transition from fast rotation to wall-locked condition a substantially irreversible process. A dedicated experimental campaign, in a wide

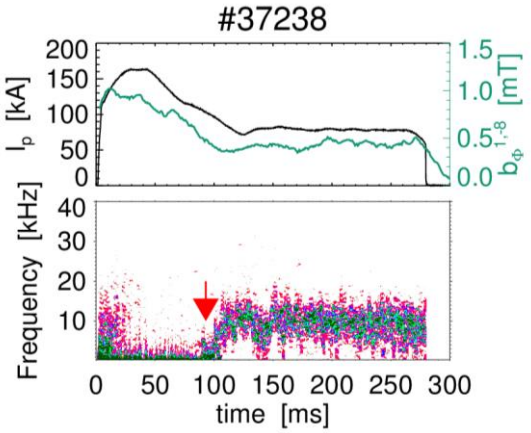

Fig. 12: top) Time traces of RFP plasma current and amplitude of the m/n=1/-8 mode; bottom) spectrogram of the 1/-8 harmonic: the unlocking threshold is overcome at around 90ms as indicated by the red arrow.

range of plasma conditions, in terms of electron density and equilibria, has shown that, in this new scenario, plasma flow rotation changes as well, being affected by the new magnetic perturbation dynamics [57].

It is worth to note that the results obtained in RFX-mod are not peculiar to the RFP, but more generally due to the feedback action itself on TM. In this sense, they are not in contradiction with those recently obtained in other RFPs, where TM locking/unlocking cycle induced by the external action of resonant magnetic perturbations exhibits hysteresis in the absence of feedback TM control.

3.2 Avoidance of m=2, n=1 tearing mode wall-locking with magnetic feedback

Experiments have been performed in RFX-mod operated as a circular, ohmic tokamak with low edge safety factor, 2<q(a)<3, to further test sophisticated feedback algorithms for the control of the m=2, n=1 TM. The experiments have demonstrated that magnetic feedback realized by active saddle coils placed outside the 100ms time-constant copper shell is able to push a wall locked m=2, n=1 mode into slow rotation with frequency of the order of several tens of Hertz. Such result has been shown to remain valid when replicated in DIII-D diverted, D-shaped, high-β plasmas, controlled by coils placed inside the 5ms time-constant vacuum vessel [58,59]. Simulations with the RFXlocking electromagnetic code indicate the improved efficiency of the feedback control with respect to the feedforward one [58].

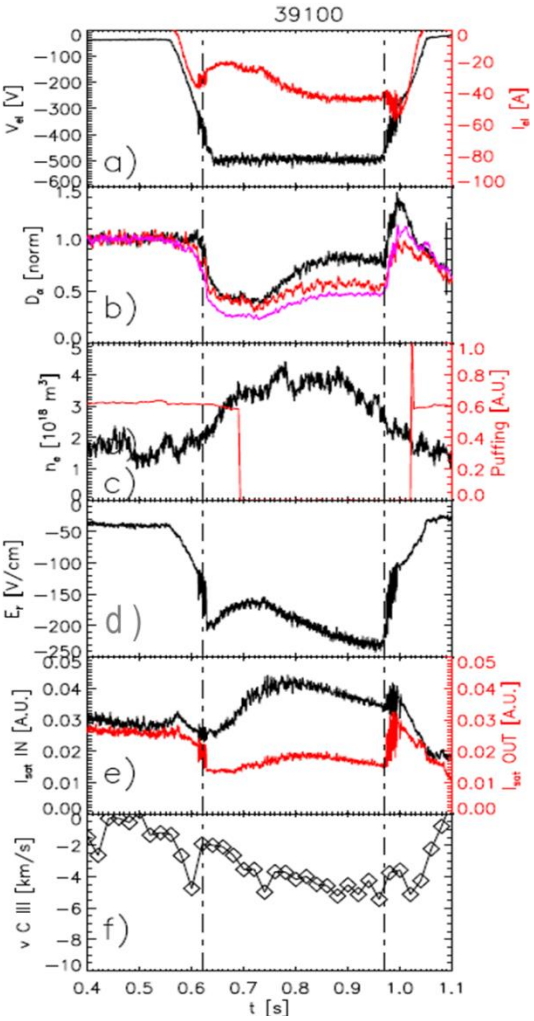

Fig. 13: Transition to high confinement example in shaped tokamak plasmas. a) applied electrode voltage and current V_{el} and I_{el}, respectively; b) D_α signals along different lines of sight (black and magenta refer to vertical lines, with an impact parameter ρ=0.24on the HFS and LFS respectively, red curve refers to an outer vertical line of sight on the LFS, ρ=0.9); c) electron density (and FB controlled puffing valve voltage); d) measured radial electric field at the edge; e) ions saturation current measured inside and outside the LFCS; f) toroidal flow velocity from CIII measurement.

4. Improved confinement scenario in the tokamak configuration

Taking advantage of its flexible system of power supplies and field shaping windings, tokamak discharges with circular and non-circular cross section can be realized in RFX-mod. It is here worth to mention that in the future also plasmas with negative triangularity could be easily produced, which have been suggested to be of interest in the control of the H-mode access [60], and extensively studied in the TCV tokamak [61].

Recently, the first enhanced confinement regimes have been obtained both in circular and single null (SN) tokamak discharges in RFX-mod thanks to the exploitation of an insertable polarized graphite electrode. The electrode has been inserted with a manipulator in various positions inside the Last Closed Flux Surface from the lower part of the device. The applied electrode voltage ranged from -800V to +350V with currents up to 300A, which allowed

inducing radial edge electric fields of both signs. For the very first time to our knowledge, edge polarization has also been tested in circular q(a)<2 discharges. Both limiter and SN discharges exhibited transitions to high confinement when the electrode was negatively polarized with respect to the first wall, which allows following and enhancing the natural radial electric field at the plasma edge. An example is shown for a Single Null discharge in Fig.13, and a similar behavior was found for circular discharges. When the applied voltage V_{el} (panel a:black trace) exceeds a threshold value and the electron density is sufficiently high, the electrode current I_{el} suddenly decreases; D_α signals, measured along different lines of sight, abruptly decrease (b); the electron density, feedback controlled thanks to newly developed algorithms [62], increases without any puffing, and the edge toroidal rotation increases as well (f); the poloidal beta and the diamagnetic energy also increase. Transition phases can be characterized by a dithering behavior. During the dithering phases, D_α, V_{el} and I_{el} signals are observed to oscillate between the low and high confinement values consistently with fast sequences of L-mode to improved confinement regime transitions and back-transitions in both circular and SN discharges. These strong fluctuations appear associated to the onset of MHD activity. The edge response to polarization has been monitored thanks to an insertable probe, measuring the floating potential, and the electron temperature and density on various radial positions. As shown in Fig. 14, the floating potential as a function of the distance from LCFS (indication of the radial electric field behavior) varies according to the polarization of the electrode and a strong electric field builds up in the few cm region within the LCFS [63,64]. The radial profile of ion saturation current, linearly depending on the electron density, steepens during transitions indicating that a local transport barrier is established, sustained by the polarized electrode [64]. Preliminary analysis of experimental data does not show clear evidence of the formation of electron temperature pedestal, so that, the steepened ion saturation profile seems to be interpreted as an indication of the formation of an electron density pedestal. It is thus unlikely that the observed improved confinement regime must be interpreted as in I-mode [65,66,67]. On the other hand, no low-frequency coherent magnetic fluctuations are measured, which are characteristic features of the so-called M-mode, as recently described [68]. It is interesting to note that, instead, various higher frequency (above 100kHz) quasi-coherent magnetic fluctuations have been identified, with ballooning and antiballooning mode structures (for more details see [69]), which closely resemble those recently described in the COMPASS tokamak in both neutral beam injector-assisted and Ohmic H-mode phases [70]. It is worth to add that, at the moment, the limitation of the experimental capabilities during tokamak operations does not allow to make closer comparison between the long lasting improved confinement regime with no bursty D_α behaviour of RFX-mod and the quiescent H-mode (QH mode) obtained in large tokamaks as a result of increased edge particle transport due to an edge harmonic oscillation [71].

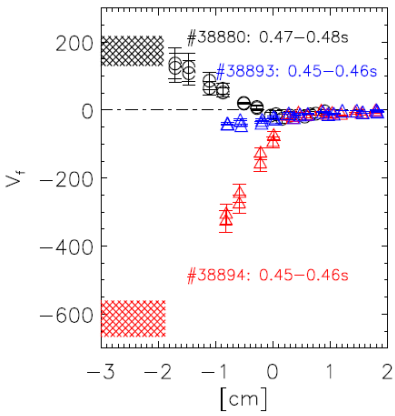

Fig.14: Floating potential edge profiles, as a function of the distance from the LCFS. Colored areas represent electrode voltage and distance from LCFS, blue points are without electrode polarization.

5. PWI interaction studies

Plasma wall interaction studies (PWI) have been performed at RFX-mod in order to investigate the behaviour under high power load of graphite, with various thermal conductivity properties, with and without the application of tungsten films. The experimental

activity was accompanied by dedicated modelling. Different tiles have been thus exposed to the RFX-mod plasma and tested by power loads up to tens of MW/m^2, in order to assess their compatibility with machine operation [72]. During experiments, the materials were inspected by visible cameras and their surface temperature was monitored by IR cameras, the power load being reconstructed thanks to a dedicated code [73]. The microscopic analysis of the retrieved samples suggested that thin films (1-3 μm) of tungsten over the same high conductivity graphite with properly smoothed surface can survive to the worst PWI conditions [72]. An example is shown in Fig. 15, where no damage of the W coating is visible after exposition to RFX-mod plasmas.

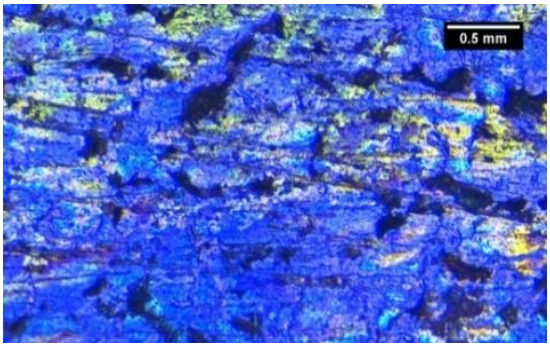

Fig. 15: Microscopic analysis of a 1 μm tungsten film on a high conductivity graphite tile exposed to RFX-mod plasmas. No damage of the metal film is seen.

Moreover, for the first time in RFX-mod, the edge transport has been analyzed and modelled exploiting thermography measurements, thanks to the IR cameras combined with an edge fluid code [73]. The measurements confirmed the presence of increased heat flux in the direction of the electron drift side, in agreement with previous RFP findings, with the interesting novelty of the identification of a density threshold above which the asymmetry disappears, comparable to that observed for the achievement of SHAx states. The modelling performed with the SOLEDGE2D-EIRENE code [74] has shown that the transport is drastically reduced in the SOL region compared to the edge one. The resulting very short heat flux decay length has important consequences on the PWI, increasing the peak power on edges of wall tiles as mentioned before

6. Proposed device upgrades

Based on the results here presented and in order to extend the explored parameter range, some enhancements for the RFX-mod device (RFX-mod2 after upgrading) have been proposed and are presently in the final design phase [75,76]. These can be summarized as:

1) upgrade of the magnetic front-end to reduce the residual magnetic chaos;

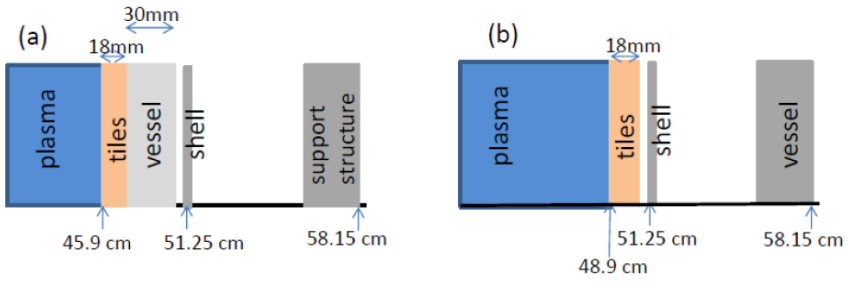

Fig. 16: (a) present layout of the magnetic front-end in RFX-mod; (b) new layout for RFX-mod2

2) change of plasma facing material (PFM) and upgrade of wall conditioning systems to improve density control and reduce wall recycling;

3) installation of a 1MW neutral beam aiming at a more reliable L-H transition in Tokamak configuration;

4) new/upgraded diagnostic systems to improve the understanding of plasma behaviour.

A reliable RFP operation at very high current requires a reduction of the localized Plasma Wall Interaction (PWI) by a decrease of the non-axisymmetric deformation of the Last Closed Magnetic Surface (LCMS) [36]. In this respect, a significant improvement of the control of the magnetic boundary was achieved in RFX-mod by the Clean Mode Control algorithm [77],

by which a reduction of the edge radial field and consequently a forced rotation of TM have been obtained, thus avoiding the stationary localized plasma wall interaction of the bulge produced by their locking in phase and to the wall. A further decrease of the residual deformation of the last magnetic surface still remains a crucial point to produce stable plasmas with stationary helical states in the 2MA range. Fig. 16a shows a sketch of the present configuration of the magnetic front-end in RFX-mod. It includes an Inconel vessel with a honeycomb structure surrounding the plasma (thickness 3.0 cm), a 0.3cm, $t_w \approx 100$ ms copper shell (radius b=51.25 cm) and a support structure (radius c=58.15 cm), the latter also supporting the control coils.

Based on simulations by the RFXLOCKING code [78], successfully used to optimize the feedback parameters in RFX-mod [79,80], it has been found that the edge radial magnetic field and the related LCMS deformation are reduced if the plasma is moved closer to the copper shell. Accordingly, the new magnetic front-end will be modified as shown in Fig. 16b: the vacuum vessel will be removed and the copper shell will become the first conductive surface for the plasma. The RFXLOCKING code has been applied to quantify the effect of such change, and the result is shown in Fig. 17, where the deformation of the LCMS is compared in the two configurations. The calculation includes the effect on m=1 modes and the impact of coil sidebands on measurements and on plasma surface distortion is taken into account. The figure indicates a reduction of a factor about 2-3 for the LCMS deformation. This simulation is performed with the pessimistic assumption that the internal amplitude of Tearing Modes will remain the same as in RFX-mod.

The new configuration will favorably impact also on m=0 modes: RFXLOCKING simulations indicate that the removal of the vacuum vessel leads by itself to a faster rotation of the LCMS bulging related to m=1 TM phase locking, which non-linearly interact with m=0 modes.

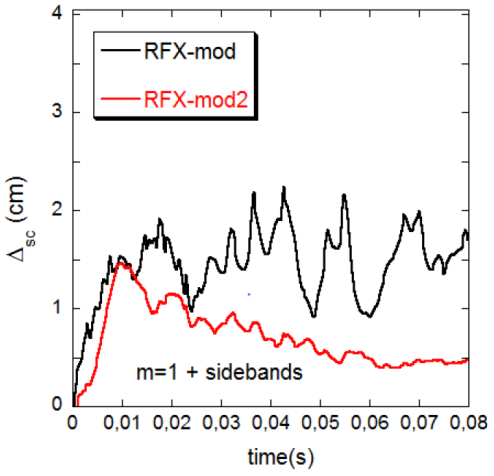

Fig. 17: deformation of LCMS, with vacuum vessel removed (red) and in present configuration (black).

In addition, the planned upgrade of the toroidal power supply system in terms of latency and synchronisation among different inverters by which it is composed will improve the effectiveness of m=0 control.

The reduction of m=0 modes is expected to have a positive effect on the robustness of helical states, because when their amplitude is kept low the non-linear coupling with secondary m=1 modes is weaker, allowing the growth of the dominant one. In addition, a better control of m=0 modes will extend the explorable density regimes, through a modification of the convective cells responsible for localized density accumulation, as described in the previous section 2.4. Finally, a better performance is expected during Pulsed Poloidal Current Drive experiments, which in the MST RFP allowed record values of the confinement time thanks to the suppression of m=0 modes [81].

The proposed change of the conductivity of the first conducting structure from Inconel to copper will have favorable consequences on the range of RFP operations with spontaneously rotating tearing modes, up to now limited to plasma current levels below 120kA, as described in section 3.1. In a numerical study conducted in [78] the locking threshold has been evaluated as a function of the conductivity of the shell located close to the plasma, with a shell to plasma radius ratio similar to the new RFX-mod2 one (RFX-mod2 will be the RFP with the highest conducting stabilizing wall, similar to MST whose wall is made by

Aluminum). This study predicts an increase of the locking threshold in terms of mode amplitude by a factor 3-5. Moreover, as already mentioned, a further increase of such threshold could be related to the decrease of mode amplitude due to the reduced shell proximity (factor 25%), leading to a new threshold in the range 375-625kA.
On the basis of the analysis on PWI summarized in section 5, for the PFC of RFX-mod2 a new shaping of the tiles has been designed, featuring a reduced flat central surface connected by rounded surface to the edges [72]. The comparison of the effect of the new shape in terms of power deposition, made by a simple calculation assuming parallel flux with an exponential decay length of 1mm (as evaluated for RFX-mod in [73]), indicates a maximum localized power load on the tile which is halved with respect to the present situation.
With regards to the first wall material, on the basis of the experimental tests mentioned in sec. 5, extruded graphite is presently the best candidate as a new tile material, because its conductivity is comparable to the Carbon Fiber Composite (CFC) one , higher by a factor about 3 than the present polycrystalline graphite tiles of RFX. It is cheaper than CFC, still maintaining suitable mechanical properties.
In order to improve the magnetic diagnostics capability and the performances of the control system during tokamak operations, a new configuration of magnetic sensors is planned for RFX-mod2, in particular with increased number of poloidal sensors, presently limited to 4 (toroidal) x 8 (poloidal) array of probes. Considering the presence of 28 tiles, an array of 12 (toroidal) x 14 (poloidal) sensors is foreseen as the minimum requirement for a measurement-based and reliable equilibrium reconstruction. This magnetic diagnostic improvement will allow a strong enhancement in the control of magnetic equilibrium and plasma shape, thus increasing the flexibility in the position of the Xpoint [82,83]; also negative triangularity shaping will be tested, as anticipated in section 4.
In tokamak configuration, the RFX-mod MHD active control system offers the opportunity for ELM mitigation and edge transport control experiments by means of RMP techniques, easily testing a variety of mode control strategies in H-mode.
To allow reliable ELMy H-mode operations, an NBI system, available at RFX (25 keV, 50 A) and originally developed at AIST (Japan) will be installed. The duration of the beam pulse, when operated at 25 keV, is limited to 30ms, which should be sufficient to induce the L-H transition, but could be short to perform RMP experiments for ELM control. However, if operated at 15 keV the pulse duration can be extended to 100 ms. Simulations by the METIS code with beam energy of 15 keV have shown that in the density parameter range of RFX-mod tokamak the losses (shine-through + orbit losses) are below 50% and scenarios with enhanced temperature and $T_i/T_e > 1$ can be explored [84]. Indeed, according to the international tokamak scaling the power threshold for a RFX-mod single-null plasma is about 0.1-0.2 MW, comparable with the ohmic power. The injection of the beam is therefore important to make the transition easier and more robust.
In addition to the upgrade of the magnetic sensor system, several new/upgraded diagnostics will be installed, to improve the understanding of the plasma behaviour and to test advanced systems providing information for applications to future devices. Among them, a new reflectometry system has been designed, based on three reflectometers located in three poloidal positions at the same toroidal angle: two on the equatorial plane, on the Low Field Side (LFS) and on the High Field Side (HFS), the third one on the upper side. In RFP, working in the O-mode, the covered density range is 3-8 x $10^{18}m^{-3}$, allowing detailed measurements of the edge density profile and, in particular, a direct probing of the HFS/LFS asymmetries and a deeper characterization of the m=0 islands. In tokamak configuration, the upper X-mode cutoff frequency will be exploited to probe the edge density both on the HFS and on the LFS; this condition is also suitable for measurements in the upper position. Main aim of the diagnostic is in this case the real-time control of plasma position, which is a critical

issue for future devices, where the use of magnetic sensors will be limited by high neutron fluxes.

7. Summary and perspectives

In the last two years the versatile RFX-mod device has been operated both as a RFP, progressing the understanding of the potentialities of this configuration, and as a tokamak, circular and shaped, exploring also the $q(a)<2$ regimes and exploiting the advanced control system for topical studies on instability mitigation by MPs. Axisymmetric and 3D helically shaped equilibria effects have been studied, the latter both spontaneous, as those obtained during SHAx states in high current RFP plasmas, and externally induced through the application of a large variety of feedback controlled magnetic perturbations.
This variety of experimental conditions allowed advancing in the understanding of the helical states with the associated transport barriers, a complete characterization of the helical edge properties of such plasmas and new studies of 3D effects on heat and particle fluxes associated to electrostatic turbulence. A more detailed analysis of the role of the majority ion mass impact on plasma performance and confinement has been performed, highlighting a 30% increase of the confinement time in Deuterium with respect to Hydrogen.
The characterization of the relation between magnetic topology and the density limit phenomenon has been advanced, exploiting the opportunity of producing $q(a) \geq 0$ plasmas. The analysis confirms the role of the m=0 chain in producing the radiative MARFE, which is no more observed when the m=0 resonance is pushed out of the plasma.
Tearing mode control studies have extended the potentiality of the feedback control to avoid dangerous 2/1 locking in tokamak plasmas and the possibility to recover the fast rotation branch also in low current RFP discharges. Suitable controlled magnetic perturbations proved to be effective in preventing runaway electron acceleration.
The first transitions to high-confinement regimes have been obtained thanks to an inserted polarized electrode in both circular and D-shaped tokamak plasmas. The formation of an edge transport barrier is monitored with edge insertable probes.
The experimental activity has been supported and stimulated by intense modelling with 3D nonlinear MHD, gyrokinetic, guiding center, transport and edge codes.
Based on the results, in order to extend the explored operational scenarios, some upgrade, not involving radical machine modifications, will be implemented, whose motivations can be summarized:

- reduction of residual magnetic chaos and achievement of more robust helical states by means of a different magnetic front-end with increased plasma-shell proximity
- improvement of density control and extension of high density regimes by means of plasma facing components optimization
- transition to H-mode in tokamak configuration by means of a better control of plasma shape (increased poloidal sensor number) and of the installation of a 1MW Neutral Beam Injector
- more effective characterization of both RFP and tokamak plasmas with innovative or improved diagnostic systems.

Acknowledgements: *The authors would like to acknowledge the invaluable support from the whole RFX-mod technical team for the operation of the machine.*

References

[1] P. Sonato et al., Fusion Eng. Des. **161**, 66–8 (2003)
[2] J.S. Sarff et al., Nucl. Fusion **53**, 104017 (2013)
[3] S. Masamune et al., "Attainment of high electron poloidal β in axisymmetric state and two routes to self-organized helical state in low-aspect-ratio RFP", IAEA-FEC25 EX/P3-52 (2014)
[4] R. Lorenzini et al., Nature Phys. **5**, 570-574 (2009)
[5] S. Cappello and D.F. Escande, Phys. Rev. Lett. 85,3838 (2000)
[6] S.Menmuir et al., Plasma Phys. Control. Fusion **52**, 095001 (2010)
[7] T.Barbui et al., Plasma Phys. Control. Fusion **57**, 025006 (2015)
[8] F.Auriemma et al., Nucl. Fusion **55**, 4 43010 (2015)
[9] R. Lorenzini et al., Phys. Rev. Lett. **116**, 185002 (2016)
[10] P. Piovesan et al., Nucl. Fusion **49**, 085036 (2009)
[11] P.W. Terry and G. G. Whelan, Plasma Phys. Controlled Fusion **56**, 094002 (2014)
[12] R. Lorenzini et al., "Transport studies with magnetic islands in fusion plasmas", Proc. 26th Int. Fusion Energy Conf. (Kyoto, Japan 17–22 October 2016) (Vienna: IAEA) EX/P5-26
[13] F. Auriemma et al., "A novel approach to the study of transport properties in plasma with magnetic islands" to be submitted for publication
[14] L. Cordaro et al., "Current sheet fragmentation after magnetic reconnection in RFP plasmas", Proc. 43rd EPS Conference on Plasma Physics, P5.015, July 2016, Leuven, Belgium
[15] S.C. Jardin, et al., Phys. Rev. Lett. **115**, 215001 (2015)
[16] D. Bonfiglio et al., "Progress in theoretical RFP studies: new stimulated helical regimes and similarities with tokamak and stellarator", Proc. 26th Int. Fusion Energy Conf. (Kyoto, Japan 17–22 October 2016) (Vienna: IAEA) TH/P3-35
[17] D. Bonfiglio, L. Chacón and S. Cappello, Phys. Plasmas **17**, 082501 (2010)
[18] D .Bonfiglio et al., Plasma Phys. Control. Fusion **57**, 044001(2015)
[19] D. Bonfiglio, S. Cappello, and D. F. Escande, Phys. Rev. Lett. **94**, 145001 (2005)
[20] L. Piron et al., "Helical flow in RFX-mod tokamak plasmas", submitted for publication
[21] P. Piovesan et al., "Role of MHD dynamo in the formation of 3D equilibria in fusion plasmas", Proc. 26th Int. Fusion Energy Conf. (Kyoto, Japan 17–22 October 2016) (Vienna: IAEA) EX/1-1
[22] U. Stroth et al., Plasma Phys. Control. Fusion **33**, 9 (1998)
[23] B.D. Scott , Phys. Fluids B **4**, 2468 (1992)
[24] M.Z. Tokar et al., Phys. Rev. Lett. **92**, 215001 (2004)
[25] I. Pustzai et al 2011 Phys. Plasmas **18**, 122501 (2011)
[26] G. Fiksel et al., Phys. Rev. Lett. **103**, 145002 (2009)
[27] M.S. Cartolano et al., Phys. Plasmas **21**, 012510 (2014)
[28] R. M. Magee et al., Phys. Rev. Lett. 107, 065005 (2011)
[29] D. Craig, et al., Rev. Sci. Instrum. **72**, 1008 (2001)
[30] B.E. Chapman et al., Phys. Plasmas 11, 2156 (2004)
[31] R. Lorenzini et al., Nucl. Fusion **55**, 043012 (2015)
[32] M. Gobbin et al., Plasma Phys. Control. Fusion **57**, 095004 (2015)
[33] M. Agostini et al., "Kinetic properties of edge plasma with 3D magnetic perturbations in RFX-mod", Proc. 26th Int. Fusion Energy Conf. (Kyoto, Japan 17–22 October 2016) (Vienna: IAEA) EX/P5-310
[34] C. Rea et al., Nucl.. Fusion **55**, 113021 (2015)
[35] N. Vianello et al., Plasma Phys. Control. Fusion **57**, 014027 (2015)
[36] M.E. Puiatti et al., Plasma Phys. Control. Fusion **55**, 124013 (2013)
[37] G. Spizzo et al, Nucl. Fusion **55** 043007 (2015)
[38] G. Pucella G. et al., Nucl. Fusion 53 023007 (2013)
[39] B. Lipschultz, J. Nucl. Mater. 145–147 15–25 (1987)
[40] O. Tudisco et al., Fusion Eng. Des. **85**, 902–9 (2010)
[41] Tokar M.Z. et al., J. Nucl. Mater. **266–269**, 958–62 (1999)
[42] M.E. Puiatti et al., Nucl. Fusion **49**, 045012 (2009)
[43] I. Predebon et al., Phys. Rev. Lett. **105**, 195001 (2010)
[44] I. Predebon and F. Sattin, Phys. Plasmas **20**, 040701 (2013)
[45] M. Zuin et al., Phys. Rev. Lett. **110**, 055002 (2013)
[46] S.F. Liu, Nucl. Fusion **54** (2014) 043006
[47] S. C. Guo, Phys. Plasmas **15**, 122510 (2008)
[48] F. Sattin et al, Plasma Phys. Controlled Fusion 52, 105002 (2010)
[49] I. Predebon et al, Phys. Plasmas **17**, 012304 (2010)
[50] S. Liu et al Phys. Plasmas **17**, 052505 (2010)
[51] D. Carmody et al, Phys. Plasmas **20**, 052110 (2013)

[52] F. Jenko, et al., Phys. Plasmas **7**, 1904 (2000)
[53] I. Predebon and P. Xanthopoulos Phys. Plasmas **22**, 052308 (2015)
[54] M. Gobbin et al., Nucl. Fusion **57,** 016014 (2017)
[55] P. Martin et al., "Physics, control and mitigation of disruptions and runaway electrons in the EUROfusion Medium Size Tokamaks science programme", Proc. 26th Int. Fusion Energy Conf. (Kyoto, Japan 17–22 October 2016) (Vienna: IAEA) EX/P6-23
[56] P. Innocente et al., Nucl. Fusion **54**, 122001 (2014)
[57] B. Zaniol et al, "Studies on RFX-mod discharges with spontaneous rotation", Proc. 42nd EPS Conference on Plasma Physics, P4.153, Lisbon, Portugal, June 2015
[58] P. Zanca et al., "Avoidance of m=2, n=1 tearing mode wall-locking by torque-balance control with magnetic feedback in DIII-D and RFX-mod", Proc. 42nd EPS Conference on Plasma Physics, P5.118, Lisbon, Portugal, June 2015
[59] P.Zanca et al., Nucl. Fusion **55**, 043020 (2015)
[60] M. Kikuchi et al., "Negative Triangularity as a Possible Tokamak Scenario", Proc. of the 12th Asia Pacific Physics Conference, JPS Conf. Proc., 015014 (2014)
[61] Y. Camenen et al., Nucl. Fusion **47**, 510 (2007)
[62] R. Cavazzana et al., "Real Time Control of Electron Density on RFX-mod Tokamak Discharges.", 20th Real Time Conference, P.96, 5-10 June 2016 Padova, Italy
[63] L. Carraro et al., "Tokamak experiments in RFX-mod with polarized insertable electrode", Proc. 43rd EPS Conference on Plasma Physics, P5.014, July 2016, Leuven, Belgium
[64] M. Spolaore et al., "H-mode achievement and edge features in RFX-mod tokamak operation", Proc. 26th Int. Fusion Energy Conf. (Kyoto, Japan 17–22 October 2016) (Vienna: IAEA) EX/P5-24
[65] R.M. McDermott et al., Physics of Plasmas **16**, 056103 (2009)
[66] D. Whyte et al., Nuclear Fusion, **50** 105005 (2010)
[67] A.E. Hubbard et al., Physics of Plasmas **18 ,** 056115 (2011)
[68] E.R. Solano et al., Nucl. Fusion **57**, 022021 (2017)
[69] M. Spolaore et al., "H-mode achievement and edge features in RFX-mod tokamak operation", submitted for publication to Nuclear Fusion
[70] A.V. Melnikov et al., Plasma Physi. Control. Fusion **57**, 065006 (2015)
[71] Xi Chen et al., Nuclear Fusion **57,** 022007 (2017)
[72] A. Canton et al., "Characterization of first wall materials in RFX-mod", Proc. 43rd EPS Conference on Plasma Physics, P5.012, July 2016, Leuven, Belgium
[73] P. Innocente et al., " Heat flux measurements and modeling in the RFX-mod experiment", Proc. 22nd PSI Conference, June 2016, Rome, Italy, P454
[74] G. Ciraolo et al., Contr. Plasma Phys. **54**, 432 (2014)
[75] M.E. Puiatti et al., "Extended scenarios opened by the upgrades of the RFX-mod experiment", Proc. 26th Int. Fusion Energy Conf. (Kyoto, Japan 17–22 October 2016) (Vienna: IAEA) EX/P5-23
[76] S. Peruzzo et al., "Design of machine upgrades for the RFX-mod experiment", presented at 29th Symposium on Fusion Technologies, Prague 5-9 September 2016, submitted Fusion Eng. Des.
[77] L. Marrelli et al Plasma Phys. Control. Fusion **49**, B359 (2007)
[78] P. Zanca, Plasma Phys. Control. Fusion **51**, 015006 (2009)
[79] L. Piron et al., Nucl. Fusion **50**, 115011 (2010)
[80] P. Zanca et al., Plasma Phys. Control. Fusion **54**, 094004 (2012)
[81] J. S. Sarff et al., Plasma Phys. contr. Fus. **45** A457-A470 (2003)
[82] G. Marchiori et al., Fusion Eng. Des. **108**, 81-91 (2016)
[83] O. Kudlacek et al., Phys. of Plasmas **22**, 102503 (2015)
[84] M. Vallar et al., "Requirements and modelling of fast particle injection in RFX-mod tokamak plasmas", presented at 29th Symposium on Fusion Technologies, Prague 5-9 September 2016, submitted Fusion Eng. Des.